ISSN 1330-3651 (Print), ISSN 1848-6339 (Online) https://doi.org/10.17559/TV-20230301000393
Original scientific paper

Comparative Energy Consumption Analysis of the Hybrid Diesel Train and the Hybrid Fuel Cell Train

Mario MIŠIĆ*, Marinko STOJKOV, Rudolf TOMIĆ, Mario LOVRIĆ

Abstract This paper compares train energy consumption of hybrid diesel-electric multiple unit (HDEMU) to hydrogen fuel-cell multiple unit (HFCMU). In the simulation, the parameters of the DMU HŽ7022 train were used for the train model created in Matlab/Simulink environment. Since the train is powered by three diesel engines in original design, it was hybridized by removing one engine and adding a battery and a supercapacitor. For comparison, a train model was made with fuel cells that have rated power of two existing diesel engines, and it was hybridized with a battery and a supercapacitor, as in the simulation with the hybridization of diesel engines. The results are presented by comparing energy consumption for both trains. In addition, voltages, electric current values and power loads of power sources are shown. As the sustainability of the system, the SOC (State of Charge) values of both the battery and the supercapacitor are presented.

Keywords: battery; diesel engine; energy consumption; fuel cell; hybrid train; supercapacitor

1 INTRODUCTION

On the basis of declared intentions on the pace of development of rail transport infrastructure, plans to electrify railway lines and targets for modal shares of rail in overall transport activity, rail activity is set to grow strongly in the Base Scenario. And yet, despite the emergence of urban and high-speed rail systems in regions of the world where these systems do not currently exist, the modal shares of passenger rail in overall transport activity stay roughly constant in the period to 2050. The share of freight transport on rail in surface freight transport falls, from 28% today to 23% in 2050. For rail to maintain current shares of passenger transport and to continue to play a role in freight supply chains substantial investment will be required. Annualized average investment in rail infrastructure worldwide would need to increase by about 50% more than levels in recent years. This will require financing at a level that will necessitate the ingenuity of many of the countries where rail can provide the most benefits [1].

Since diesel engines pollute the environment a lot, one possibility is to reduce harmful exhaust gas emissions or eliminate them completely. Harmful exhaust gas emissions from transport are increasing due to the increase in passengers and freight traffic [2]. Reducing harmful exhaust gas emissions can be achieved by downsizing engines that meet Euro 6 standards [3] or by hybridization [4]. Downsizing engine is not considered in this paper, but hybridization is covered.

Elimination of harmful gas emissions is possible only if some other fuel power source is installed instead of the diesel engine. Such a device is for example here used -a proton-exchange membrane fuel cell (PEMFC), also known as polymer electrolyte membrane fuel cell. This type of fuel cell can achieve high efficiency and can work without harmful gas emissions. PEMFC use hydrogen as a fuel that can be produced from renewable energy sources. PEMFC has a simple construction, quick start and response, and high-power density (kW/kg), which makes it suitable as a power source in railway vehicles. The PEMFC is usually fed by hydrogen and oxygen from providing a clean process with water as the only secondary product. When used in conjunction with an electric motor it provides clean and virtually noise free form of railway transportation [5].

For better energy saving, the PEMFC railway vehicle can be hybridized with batteries that will be able to be charged by recuperation of regenerative braking energy. Optimal size selection of a hybrid energy system including lithium-ion battery and PEMFC can supply the driving force of a locomotive. The main purpose is to minimize the total cost of system with different constraints including the capacity constraint of the battery and the state-of-charge limit [6]. The fuel cell hybrid locomotive system consists of PEMFC, DC/DC converter, battery energy store system, three-phase asynchronous traction motor, traction inverter as main components and in that topology the storage battery is utilized to supplement the output power of the PEMFC during locomotive acceleration and cruise and is used for recuperation of regenerative braking energy [7, 8].

As an improvement in energy storage and fuel economy, a supercapacitor can be added. The supercapacitor has a much faster response than the battery and PEMFC, also can help with traction and recuperation of regenerative braking energy. When a train accelerates, it absorbs a large amount of power to create the required power needed for maintaining the desired speed. Unlike batteries, a supercapacitor will have more charge and discharge cycles due to its faster response [9].

A double-layer electrochemical supercapacitor can store thousand times more energy than a typical capacitor. It shares the characteristics of both batteries and conventional capacitors and has an energy density about 20% of a battery. Moreover, they have almost negligible power losses and long lifespan [10].

2 TOPOLOGY OF TRACTION SYSTEM

The topology used for traction hybrid system for rail cars is connected in series [11]. The HDEMU traction system topology uses two diesel engines (DE), an alternator (AL) with a rectifier (RF), a battery (B) with a bidirectional DC/DC converter (BDC), a supercapacitor (SC) with a bidirectional DC/DC converter (BDC), an insulated gate bipolar transistor (IGBT) and three-phase asynchronous traction motors (AM). For the HFCMU, the topology is very similar, except that instead of a diesel engine, the main power source is provided by PEMFC connected to a DC/DC converter (ODC). With this topology, traction motors always receive three-phase current via IGBT from any power source (Fig. 1).

Topology requires an energy management unit for proper work. Under full load, the diesel engine (fuel cell), supercapacitor and battery participate in the traction of the train. During cruising, the energy management first discharges the supercapacitor and then the battery. Also, at that moment diesel engines are idle for the HDEMU, equivalent to the PEMFC for the HFCMU. With recuperation of regenerative braking energy, the management unit first directs the energy to charge the supercapacitor at first and then to the battery (Fig. 2).

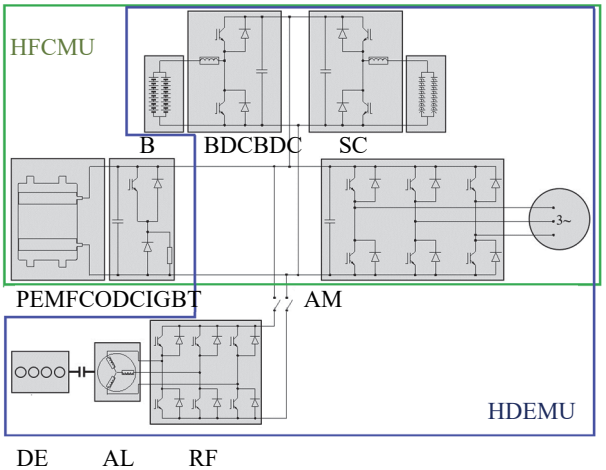

Figure 1 Topology of HDEMU and HFCMU [11]

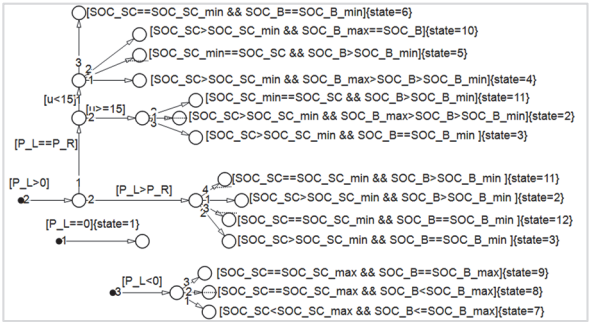

Figure 2 Energy management

3 MODELING OF RAILWAY TRACK

The simulation is performed according to the parameters of the real railway in Croatia between Knin and Perkovic with a length of 53,71 km (Fig. 3).

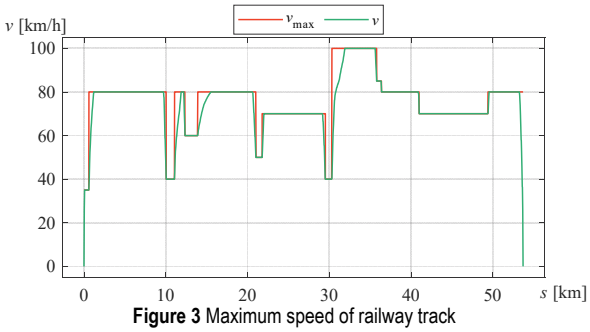

Figure 3 Maximum speed of railway track

The railway section belongs to the international railway line M604 Ostarije - Knin - Split. The railway is hilly with a lot of gradients, where the recuperation of regenerative braking energy will come to the fore. The highest gradient is 25,5‰ (Fig. 4) and the smallest curvature radius of the railway track is 215 m (Fig. 5).

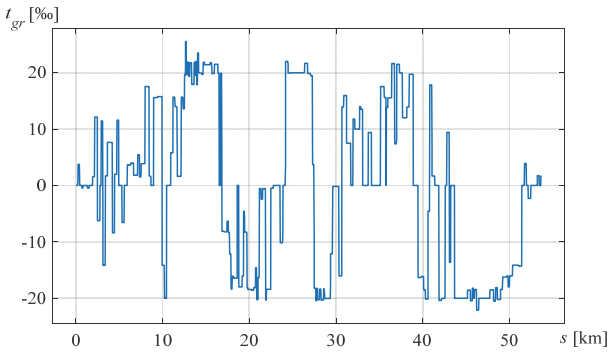

Figure 4 Gradient of railway track

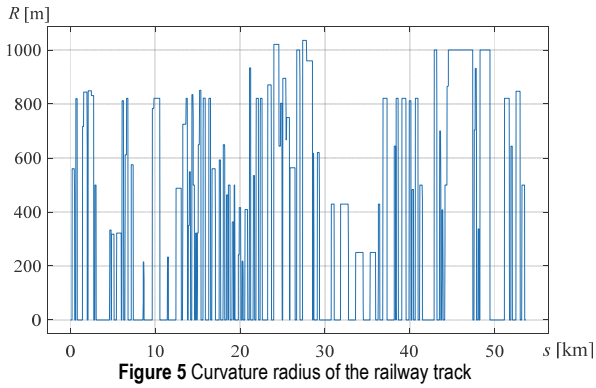

Figure 5 Curvature radius of the railway track

4 TRAIN MOTION MODEL

The aim of the simulation model is the calculation of energy and fuel consumption obtained by integrating power. The simulation model uses train parameters such as tractive and braking power, maximum speed and mass, and calculates traction effort and motion resistance force using track parameters. Acceleration, speed and the distance traveled by the train result from all of this. The simulation model determines at each time step the acceleration $a(t)$ (deceleration $-a(t)$), the speed $v(t)$ and the position $s(t)$ of the train using the equations of motion:

$$a(t) = \frac{1}{m_{\text{tot}}}(F_{\text{tr}} - F_{\text{res}}) \tag{1}$$

$$v(t) = \int a\,\mathrm{d}t \tag{2}$$

$$s(t) = \int v\,\mathrm{d}t \tag{3}$$

where m_{tot} is the total mass of the train in tonnes increased by 6% due to the inertia of the rotating masses [12], F_{tr} is the traction force on wheels in kN and F_{res} train is the resistance force in kN:

$$F_{\text{res}} = F_{\text{dr}} + F_{\text{gr}} + F_{\text{cu}} \tag{4}$$

where F_{rr} is the rolling resistance force of the train in kN, F_{gr} is the resistance force on the track gradient in kN and F_{cu} is the track curvature resistance force in kN. For decceleration:

$$a(t) = (-F_{\text{br}} - F_{\text{res}}) / m_{\text{tot}} \tag{5}$$

where F_{br} is the braking effort on wheels in kN.

Traction effort is a function of constant torque and constant power transmitted to the wheels from the traction motor:

$$F_{tr} = \begin{cases} F_{tr} = F_{tr,max} \ \forall v \le v_{cr} \\ F_{tr} = P_{tr,max} \cdot v^{-1} \ \forall v > v_{cr} \end{cases} \quad (6)$$

also, for braking effort:

$$F_{br} = \begin{cases} F_{br} = F_{br,max} \ \forall v \le v_{cr} \\ F_{br} = P_{br,max} \cdot v^{-1} \ \forall v > v_{cr} \end{cases} \quad (7)$$

where $F_{tr,max}$ is the maximum traction force, $P_{tr,max}$ is the maximum traction power, $F_{tr,max}$ is the maximum braking power, $F_{br,max}$ is the maximum braking force, $P_{br,max}$ is the maximum braking power and v_{cr} is the train critical speed.

The rolling resistance force of the train is [13]:

$$F_{rr} = r_r + r_p \cdot v + r_a \cdot v^2 \quad (8)$$

where r_r is the rolling resistance force in kN, r_p is the resistance coefficient of parasitic movements in kN/kmh^{-1}, r_a is the air resistance coefficient in kN/(kmh^{-1})^2.

The resistance force on the track gradient is:

$$F_{gr} = m_{tot} \cdot g \cdot t_{gr} \cdot 10^{-3} \quad (9)$$

where t_{gr} is the gradient of the railway track in ‰.

The track curvature resistance force is:

$$F_{cu} = \frac{m_{tot} \cdot g}{2(R-30)} \quad (10)$$

where R is the radius of curvature of the railway track in m.

The consumed power on wheels should be:

$$P_{Load} = \begin{cases} P_{Load} = F_{tr} \cdot v(t) \ \forall \ F_{tr} \ge F_{res} \\ P_{Load} = F_{br} \cdot v(t) \ \forall \ F_{br} < 0 \end{cases} \quad (11)$$

5 TRACTION MOTOR MODEL

The traction motor transmits power with losses. Losses will be affected due to the different operating points of the traction motor depending on the rotation speed (rpm). Also, the traction motor provides power through the gear box to wheels with losses. Therefore, the power of the traction motor is defined as:

$$P_{Load} = \begin{cases} P_{Load} = P_{Load,TM} \cdot \eta_{TM} \cdot \eta_{red} \ \forall \ F_{tr} \ge F_{res} \\ P_{Load} = \dfrac{P_{Load,TM}}{\eta_{TM} \cdot \eta_{red}} \ \forall \ F_{br} < 0 \end{cases} \quad (12)$$

where $P_{Load,TM}$ is the power of the traction motor, η_{TM} is the efficiency of the traction motor (Fig. 6) and η_{red} is the efficiency of the reducer with gearbox (Fig. 7).

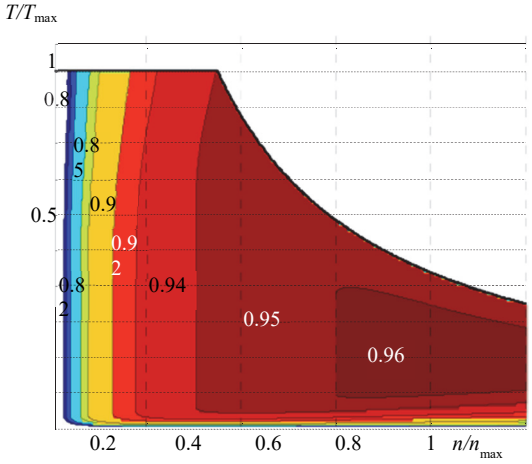

Figure 6 Efficiency of the traction motor [14]

Since the efficiency of the traction motor is determined by the torque, it should be calculated:

$$T_{TM} = P_{TM} \cdot \omega_{TM} \quad (13)$$

where ω_{TM} is the angular velocity of the traction motor:

$$\omega_{TM} = \omega_{wh} \cdot gr = \frac{2v}{D_{wh}} \cdot gr \quad (14)$$

where D_{wh} is the wheel diameter and gr is the gear ratio.

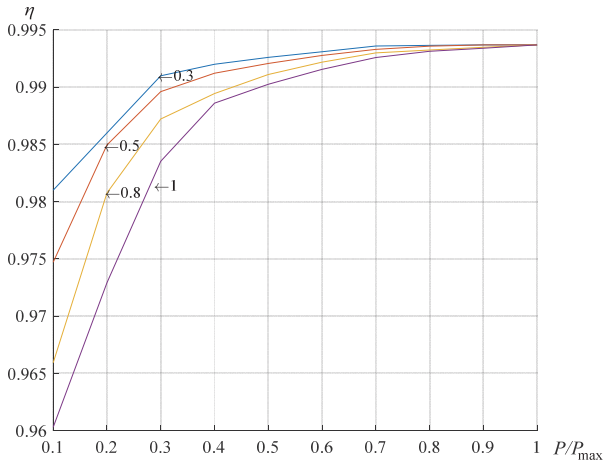

Figure 7 Efficiency of the reducer [15]

6 TRACTION INVERTER MODEL

The traction inverter manages the power of the power sources, combines them during traction and converts the DC power into a three-phase alternating current. Traction inverters perform functions such as voltage boosting, switch protection and regenerative braking. The converter is made in IGBT technology. The converter contains control circuits and computers for monitoring the operation of the converter and drive as a whole ("converter computer" and "superior traction computer") so that in addition to the basic function of powering the traction motors, the converter also performs the functions of monitoring and protecting the power drive and communicating with the superior computer inside a train system which power sources and with a brake subsystem.

In this case, the traction inverter is an insulated-gate bipolar transistor (IGBT) and will provide power:

$$P_{\mathrm{TI}} = \begin{cases} P_{\mathrm{TI}} = P_{\mathrm{DC}} \cdot \eta_{\mathrm{TI}} \ \forall \ F_{\mathrm{tr}} \geq F_{\mathrm{res}} \\ P_{\mathrm{TI}} = P_{\mathrm{DC}} \cdot \eta_{\mathrm{TI}}{}^{-1} \ \forall \ F_{\mathrm{br}} < 0 \end{cases} \tag{15}$$

where P_{DC} is the DC/DC converter power and η_{TI} is the efficiency of the traction inverter (Fig. 8).

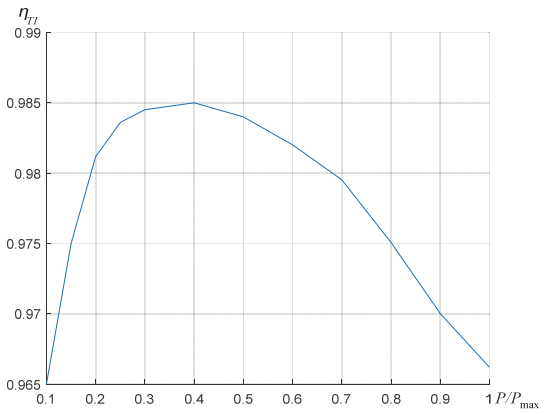

Figure 8 The traction inverter efficiency with rectifier [16]

7 MODELING OF THE DC/DC CONVERTER

The bidirectional DC/DC converter increases the voltage from the direct current power source from 800 V to the voltage for the main circuit of the IGBT to 2,4 kV at the time of train traction [17]. Since the converter is bidirectional, when the train brakes, the power travels in the opposite direction, reducing the voltage and supplying current to the power sources. A chopper, a converter in one direction, is used to increase the FC voltage. Since current cannot be transferred to the FC or the diesel engine, no bidirectional converter is required. Power at a converter for HDEMU is:

$$P_{\mathrm{DC}} = \begin{cases} P_{\mathrm{DC}} = (P_{\mathrm{DE}} + P_{\mathrm{SC}} + P_{\mathrm{B}}) \cdot \eta_{\mathrm{DC}} \ \forall \ F_{\mathrm{tr}} \geq F_{\mathrm{res}} \\ P_{\mathrm{DC}} = (P_{\mathrm{FC}} + P_{\mathrm{SC}} + P_{\mathrm{B}}) \cdot \eta_{\mathrm{DC}} \ \forall \ F_{\mathrm{tr}} \geq F_{\mathrm{res}} \\ P_{\mathrm{DC}} = (P_{\mathrm{SC}} + P_{\mathrm{B}}) \cdot \eta_{\mathrm{DC}}{}^{-1} \ \forall \ F_{\mathrm{br}} < 0 \end{cases} \tag{16}$$

where P_{DE} is the diesel engine power, P_{SC} is the supercapacitor power, P_{B} is the battery power, P_{FC} is the fuel cell power and η_{DC} is the efficiency of the DC/DC converter (Fig. 9).

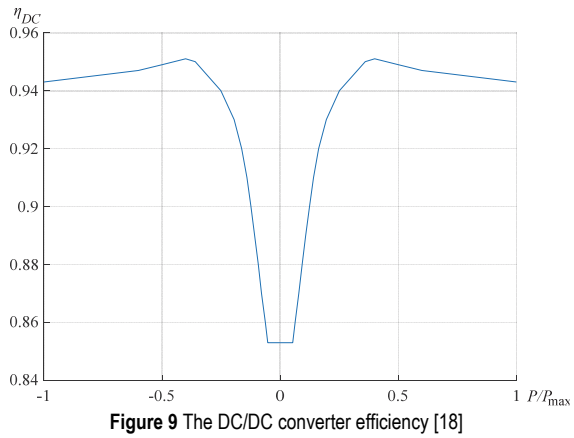

Figure 9 The DC/DC converter efficiency [18]

8 MODELING OF THE DIESEL ENGINE AND THE ALTERNATOR WITH THE RECTIFIER

The diesel engine (DE) operates in two modes: full load and idle. Since the DE is connected by a rigid clutch to the alternator, it will spin at the same rpm as the rigid clutch. It spins at 1200 rpm at idle, and 2000 rpm at full load.

The power provided by the power source, in this case the diesel engine, will be transmitted to the wheels of the train with losses. Since the DE must rotate at the rated speed of the alternator, the rated power of the DE is calculated as:

$$P_{\mathrm{DE}} = P_{\mathrm{DE,max}} \cdot \eta_{\mathrm{rpm}} \tag{17}$$

where η_{rpm} is the ratio of maximum power to rated power with regard to the number of revolutions (rpm) of alternator and $P_{\mathrm{DE,max}}$ maximum power (Fig. 10).

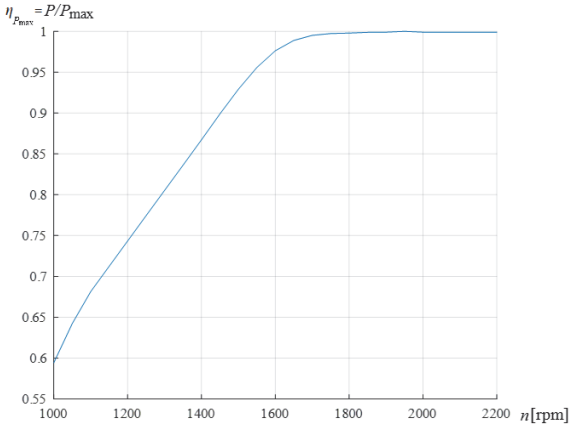

Figure 10 Ratio of the maximum power to the rated power

Energy consumption in a diesel engine is defined as:

$$E_{\mathrm{DE}} = W_{\mathrm{DE}} = \int P_{\mathrm{DE}} \mathrm{d}t \tag{18}$$

while diesel fuel consumption is:

$$V_{\mathrm{df}} = \frac{E_{\mathrm{DE}} \cdot g_{\mathrm{e}}}{\rho_{\mathrm{df}}} \tag{19}$$

where ρ_{df} is the diesel fuel density, g_{e} is the specific effective diesel fuel consumption given by the manufacturer [19, 20].

The output power from the alternator with the rectifier is connected to main circuit and it should be:

$$P_{\mathrm{AL}} = P_{\mathrm{DE}} \cdot \eta_{\mathrm{AL}} \cdot \eta_{\mathrm{RF}} \tag{20}$$

where η_{AL} is the alternator efficiency [21] and η_{RF} is the rectifier efficiency (Fig. 8).

In traction, the diesel engine participates with the hybridization ratio:

$$HR_{\mathrm{DE}} = \frac{P_{\mathrm{DE}} \cdot \eta_{\mathrm{TI}}}{P_{\mathrm{DC}}} \tag{21}$$

9 MODELING OF THE PEMFC

PEMFCs are static energy conversion devices which convert directly the chemical energy of fuel into DC electrical energy. The main advantages of the PEMFCs are: high efficiency, low or zero emissions when hydrogen is used as a fuel, low noise during operation and high modularity.

The PEMFC is considered one of the most promising technologies for application in hybrid vehicles due to its high-power density, low operating temperature, a certain level of rather quick startup capability, and long-life time [22].

The stack voltage is multiplied voltage of single cell of PEMFC by number of cells n_{cell} [23]:

$$U_{\text{FC,st}} = n_{\text{cell}}(E - U_{\text{act}} - U_{\text{ohm}} - U_{\text{con}}) \tag{22}$$

where E is Nernst potential:

$$E = 1,229 - 8,5\cdot10^{-4}(T - 298,15) + \\ +4,308\cdot10^{-5}T(\ln p_{\text{H}_2} + 0,5\ln p_{\text{O}_2}) \tag{23}$$

where T is the temperature of the cell, p_{H2} partial pressure of hydrogen and p_{O2} partial pressure of oxygen, while U_{act}, U_{ohm} and U_{con} are polarization losses of voltage described by:

$$U_{\text{act}} = -0,9514 + (31,2 - 1,87\ln i_{\text{FC}} + 7,4\ln C_{\text{O}_2})\cdot10^{-4}T \tag{24}$$

$$U_{\text{ohm}} = -1,605\cdot10^{-2}i_{\text{FC}} + 3,5\cdot10^{-5}T\cdot i_{\text{FC}} - 8\cdot10^{-5}{i_{\text{FC}}}^2 \tag{25}$$

$$U_{\text{con}} = 0,016\ln(1 - \frac{i_{\text{FC}}}{i_{\text{lim}}}) \tag{26}$$

where T is the temperature of cell, i_{FC} is the current of the PEMFC load, i_{lim} is limited current and C_{O2} the oxygen concentration:

$$C_{\text{O}_2} = \frac{p_{\text{O}_2}}{5,08\cdot10^6}\text{e}^{\frac{498}{T}} \tag{27}$$

$$p_{\text{H}_2} = 0,5(p_{\text{a}}\text{e}^{\frac{-1,635\cdot i}{A\cdot T^{1,334}}} - p_{\text{H}_2\text{O}}^{sat}) \tag{28}$$

$$p_{\text{O}_2} = p_{\text{c}}\text{e}^{\frac{-4,192\cdot i}{A\cdot T^{1,334}}} - p_{\text{H}_2\text{O}}^{sat} \tag{29}$$

where $p_{\text{a}} = 2$ bar is the anode partial pressure, $p_{\text{c}} = 1$ bar is the cathode partial pressure [23], $A = 882$ cm^2 and the water saturation pressure:

$$p_{\text{H}_2\text{O}}^{\text{sat}} = 10^{-2,18+2,95\cdot10^{-2}(T-273,15)-} \\ -9,18\cdot10^{-5}(T-273,15)^2+1,44\cdot10^{-7}(T-273,15)^3 \tag{30}$$

The PEMFC power is:

$$P_{\text{FC}} = \frac{P_{\text{DC}}}{\eta_{\text{DC}}}\cdot HR_{\text{FC}}\cdot\eta_{\text{FC}} = U_{\text{FC}}\cdot I_{\text{Load,FC}}\cdot\eta_{\text{FC}} \tag{31}$$

$$I_{\text{Load,FC}} = i_{\text{FC}} = \frac{P_{\text{DC}}\cdot HR_{\text{FC}}}{\eta_{\text{DC}}\cdot U_{\text{FC}}\cdot\eta_{\text{FC}}} \tag{32}$$

where HR_{FC} is the fuel cell hybridization ratio which is equalized to diesel engine hybridization ratio, η_{FC} is the PEMFC efficiency (Fig. 11) and U_{FC} the fuel cell total voltage:

$$U_{\text{FC}} = n_{\text{st}}\cdot n_{\text{mo}}\cdot U_{\text{FC,st}} \tag{33}$$

where n_{st} is the number of stacks and n_{mo} is the number of modules.

Energy consumption in a fuel cell is defined as:

$$E_{\text{FC}} = \int P_{\text{FC}}\text{d}t \tag{34}$$

and hydrogen consumptionis defined as:

$$m_{\text{H}_2} = E_{\text{FC}}\cdot H_{\text{LHV}} \tag{35}$$

where H_{LHV} is the hydrogen lower heating value.

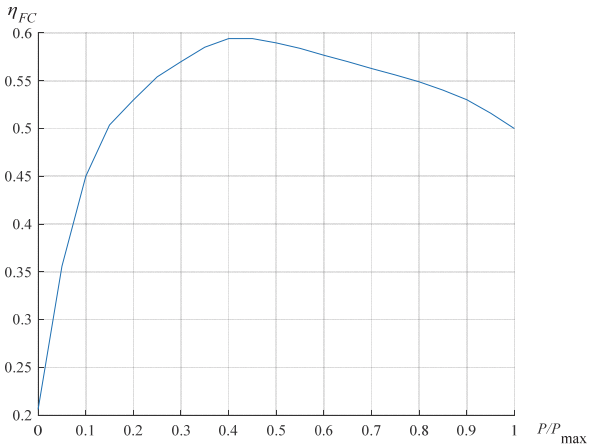

Figure 11 Fuel cell efficiency [24]

10 MODELING OF THE BATTERY

Li-ion batteries are named after the material from which the cathode is made, while iron phosphate proved to be the best anode. Batteries are sensitive to overcharging and over discharging, so in terms of safety today, the safest type is a LiFePO4 (LFP).

The voltage of the single cell of the LFP battery is 3,2 V. By connecting cells in series, the desired voltage is obtained, and by connecting cells in series, the desired capacity is obtained. To preserve the battery, state of charge (SOC) should be kept between 20% and 80%.

Battery cell voltage at discharge is [25]:

$$U_{\text{B}} = E_0 - K\frac{Q_{\text{B}}}{Q_{\text{B}} - i_{\text{B}}\cdot t}i_{\text{B}}\cdot t - K\frac{Q_{\text{B}}}{Q_{\text{B}} - i_{\text{B}}\cdot t}i_{\text{B}} - \\ -R_{\text{B}}\cdot i_{\text{B}} + A\text{e}^{-B\cdot i_{\text{B}}\cdot t} \tag{36}$$

where E_0 is the constant voltage, K is the polarization constant or the polarization resistance, Q_B is the standard battery capacity, i_B is the battery current load, R_B is the battery internal resistance, A is the voltage drop during the exponential zone and B is the exponential zone time constant inverse.

Battery cell voltage at charge is:

$$U_B = E_0 - K\frac{Q_B}{Q_B - i_B \cdot t} i_B \cdot t - K\frac{Q_B}{i \cdot t - 0.1Q_B} i_B - \\ -R_B \cdot i_B + A e^{-B \cdot i_B \cdot t} \quad (37)$$

The constant voltage is:

$$E_0 = U_{max} + K + R_B \cdot i_B - A \quad (38)$$

where A is the exponential amplitude:

$$A = U_{max} - U_{exp} \quad (39)$$

The polarization constant or the polarization resistance is [26]:

$$K = (U_{max} - U_{nom} + A(e^{-B \cdot Q_0} - 1))(\frac{Q_B}{Q_{nom}} - 1) \quad (40)$$

where Q_{nom} is the nominal capacity at the nominal voltage U_{nom}.

The battery power is:

$$P_B = \frac{P_{DC}}{\eta_{DC}} \cdot HR_B = n_{s,B} \cdot U_B \frac{I_{Load,B}}{n_{p,B}} \quad (41)$$

$$I_{Load,B} = i_B = \frac{P_{DC} \cdot HR_B \cdot n_{p,B}}{\eta_{DC} \cdot U_B \cdot n_{s,B}} \quad (42)$$

where $n_{s,B}$ is the number of serial cells, and $n_{p,B}$ is the number of parallel cells of the battery.

State of charge is calculated as:

$$SOC_B = 1 - Q_B^{-1} \int i_B dt \quad (43)$$

11 MODELING OF THE SUPERCAPACITOR

Supercapacitors have an energy density per unit volume of 10 Wh/L to 50 Wh/L, which is smaller than a battery, but contains a high output density and a long service life. It also provides excellent properties when working at higher temperatures, but self-discharge is more pronounced than with a LFP battery.

Their lifetime is usually greater than 500 000 cycles at 100% discharge (as opposed to batteries that are discharged to 80%), while their lifetime can exceed 12 years [27]. In addition, the supercapacitor can be easily charged and discharged in seconds and its energy efficiency is very high, ranging from 85% to 98%. Due to these properties, it is suitable as a power source for additional hybridization.

The voltage of the supercapacitor power source is [10]:

$$U_{SC} = n_{s,SC}(U_1 + R_1 \cdot I_{SC}) \quad (44)$$

where $n_{s,SC}$ is the number of serial cells and $n_{p,SC}$ is the number of parallel cells of the supercapacitor power source, also R_1 is the resistance of the main cell, I_{SC} is the load current and U_1 is the voltage of the main cell as well described:

$$U_1 = \frac{-C_0 + \sqrt{C_0^2 + 2C_v \cdot Q_1}}{C_v} \quad (45)$$

where C_0 is the constant capacitance, C_v is the constant parameter and Q_1 is the instantaneous charge of C_1 in main cell calculated by:

$$Q_1 = C_0 \cdot U_1 + 0.5C_v \cdot U_1^2 \quad (46)$$

The voltage of the slow cell is [10]

$$U_2 = \frac{1}{C_2}\int i_2 dt = \frac{1}{C_2}\int \frac{1}{R_2}(U_1 - U_2)dt \quad (47)$$

where C_2 is the capacitance and R_2 is the resistance of the slow cell.

The supercapacitor power is:

$$P_{SC} = \frac{P_{DC}}{\eta_{DC}} HR_{SC} = U_{SC} \frac{I_{Load,SC}}{n_{p,SC}} \quad (48)$$

$$I_{Load,SC} = i_{SC} = \frac{P_{DC} \cdot HR_{SC} \cdot n_{p,SC}}{\eta_{DC} \cdot U_{SC}} = i_1 + i_2 \quad (49)$$

where $n_{p,SC}$ is the number of parallel cells.

State of charge is defined as:

$$SOC_{SC} = 1 - Q_{SC}^{-1} \int i_{SC} dt \quad (50)$$

12 TECHNICAL DESCRIPTION OF POWER SOURCES

In a HDEMU two Diesel engines "MAN" D 2842 LE622 for railway vehicles are used and in a HFCMU nine PEMFC modules "Ballard" FC velocity-HD6 are used.

For hybridization rechargeable LFP battery "LithiumWerks" 26650 and "Maxwell" supercapacitor BCAP3000 are used.

Table 1 Properties of power sources

Diesel engine	
Rated maximum power, $P_{DE,,max}$	588 kW
Rated engine speed, n	1800 rpm
Idle engine speed, n_{id}	600 rpm
Average specific fuel consumption, g_e	211 g/kWh
Mass, m_{DE}	1480 kg
Fuel cell	
Rated power, P_{FC}	150 kW
Idle power, $P_{FC,min}$	6 kW
Nominal voltage, U_{FC}	800 V
Maximum load current, $I_{FC,max}$	320 A
Average hydrogen consumption, q_{H2}	2,5 g/s
Mass, m_{FC}	404 kg

Table 2 Properties of power sources (continuation)

Battery	
Nominal module voltage, $U_{B,mod}$	800 V
Rated voltage, U_0	3,3 V
Rated capacity, Q_0	2,56 Ah
Charging current, I_{CH}	10 A
Discharging current, I_{DIS}	6,5 A
Mass, m_B	76 g
Supercapacitor	
Nominal module voltage, $U_{SC,mod}$	800 V
Nominal capacitance, C_{SC}	3000 F
Discharging current, I_{DIS}	150 A
Rated voltage, U_{SC}	2,7 V
Mass, m_{SC}	506,7 g

13 RESULTS AND DISCUSSION

If the rated power of the remaining two engines (2 × 588 kW) is subtracted from the total HDEMU power, 33% will be lost to battery/supercapacitor hybrid power sources. The simulation was performed in two cases so that the battery takes 25% and 40% of hybridization in relation to the supercapacitor. For the HFCMU, the power of the fuel cells is set according to the factory module of the PEMFC 9 × 150 kW. In both two analysed cases, *SOC* of batteries and supercapacitors, fuel and energy consumption are observed.

If the hybridization ratio is HR_B/HR_{SC} = 0,25/0,2, the energy is distributed almost equally between the battery and the supercapacitor. In this case, for both HDEMU and HFCMU, the *SOC* of the batteries will come to 0,2 and thus the power is judged on the fuel cell. Although the algorithm does not allow $SOC_B = 0$, such deeper discharges will still affect its life. For this hybridization ratio HDEMU will consume 162,419 L of fuel and HFCMU 9,442 kg of hydrogen (Fig. 12 and Fig. 15). Since the supercapacitor has a fast response, it charges and discharges several times compared to the battery and do not affect the service life of the supercapacitor. The supercapacitor works in the range of $1 < SOC_{SC} < 0{,}02$. If an attempt is made to reduce the hybridization ratio of the battery below 25%, the fuel cell overheats and thus this is the lowest possible hybridization ratio of the battery (Fig. 13 and Fig. 16).

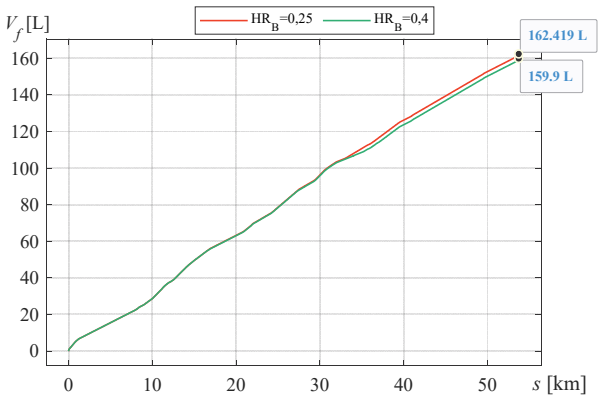

Figure 12 Diesel fuel consumption in liters (L)

According to the hybridization ratio and the strength of the discharge current of the battery and the supercapacitor, the cells are combined into packs. For the battery pack, it will be needed to connect 243 cells in a series and 87 cells in parallel, totally 21 141 cells. For a supercapacitor pack, 296 cells will be needed to connect in series and 4 cells in parallel, totally 1 148 cells. The battery pack and the supercapacitor pack together are lighter than a single diesel engine and alternator, thus maintaining the mass of a classic train.

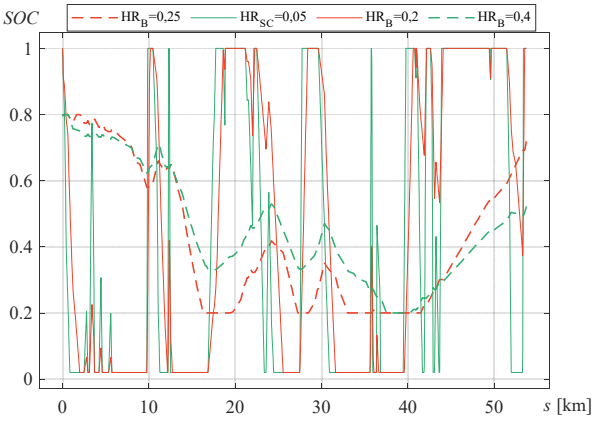

Figure 13 SOC distribution of HDEMU

In the case of increasing the hybridization ratio of the battery up to HR_B/HR_{SC} = 0,4/0,05, the battery enters the state SOC_B = 0,2 only once with HDEMU and never with HFCMU (Fig. 13 and Fig. 16). By avoiding deep discharge, the life and degradation of the battery is extended. In this case, there will be fuel savings and the HDEMU will consume 159,9 L of fuel (Fig. 12). This hybridization ratio also reduces hydrogen consumption in HFCMU to 9,256 kg (Fig. 15). For the battery pack, it will be needed to connect 243 cells in a series and 139 cells in parallel, totally 33 777 cells. For a supercapacitor pack, 296 cells will be needed to connect in series and 1 cell in parallel, totally 296 cells. The battery pack and the supercapacitor pack together are almost same mass as a single diesel engine and alternator.

The theoretical sum of energy of all devices for the lowest fuel (hydrogen) consumption shows the main difference between HDEMU and HFCMU. Since the idle speed of the diesel engine is at 68% of the rated power, and of the fuel cell at only 4%, the savings are more pronounced in the HFCMU than in the HDEMU. It can be seen that the total energy consumption of the HDEMU is 678,497 kWh, and the diesel engine alone consumes 667,678 kWh (Fig. 14). Regenerative braking did not result in savings, but it can be said that by replacing one engine of a classic train with energy storages, the fuel consumption of the third engine is completely eliminated, and the lack of energy is replaced by battery storage.

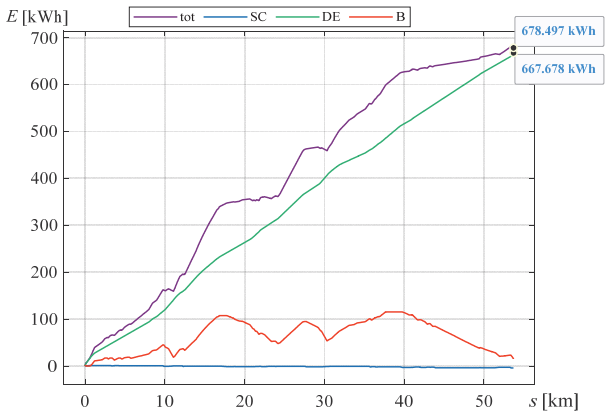

Figure 14 Energy distribution with minimal fuel consumption of HDEMU

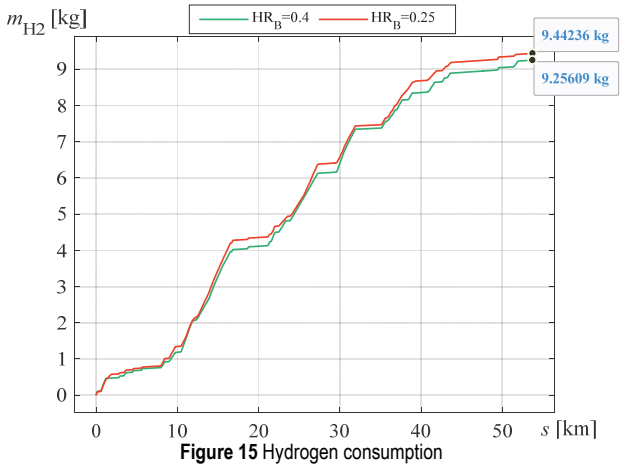

Figure 15 Hydrogen consumption

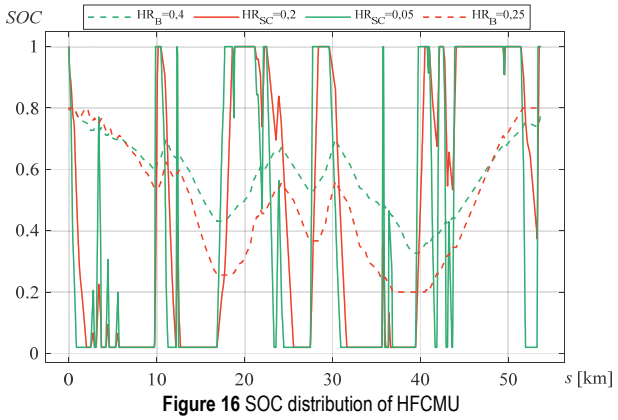

Figure 16 SOC distribution of HFCMU

Due to the large difference in idle and rated power of the fuel cell, regenerative braking comes to the fore and savings are created. The theoretical sum of energy of all power sources for the lowest hydrogen consumption is 277,984 kWh, and the energy consumption of the fuel cell is 311,107 kWh (Fig. 17). It can be concluded that energy was saved by regenerative braking and at the end of the train drive the battery and the supercapacitor were additionally charged.

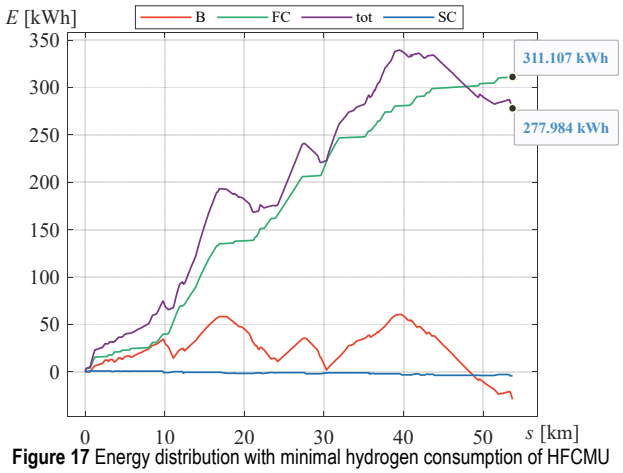

Figure 17 Energy distribution with minimal hydrogen consumption of HFCMU

By decreasing the hybridization ratio of the battery, the SOC_B decreases, the battery is more loaded, and the SOC_{SC} changes in negligible limits.

Comparing the prices of today's market, it must be known that classic vehicles with diesel engines are still the cheapest. But despite higher prices, hybrid diesel motor unit is still not more profitable than hybrid fuel cell train (Tab. 3).

Table 3 Price comparison of train power devices

		Number of units		
	Price / €	DMU	HDEMU	HFCMU
Diesel engine	25 000	3	2	0
Alternator	12 000	3	2	0
Inverter	35 000	3	3	3
Converter	25 000	0	2	3
Battery	5	0	33777	33777
Supercapacitor	90	0	296	296
Fuel cell	60 000	0	0	9
Total / €		216 000	424 525	375 525

14 CONCLUSION

A comparative energy consumption of hybrid diesel electric multiple unit and hybrid fuel cell multiple unit has been analyzed and fuel consumption is shown. Since the energy and fuel consumption is higher for HDEMU than HFCMU and it is obvious that in terms of environmental protection, the fuel cell has a great advantage over the diesel engine.

Because the railway track is sharp and demanding, the energy management had to be different than what is usually set. Big uphills consume a lot of energy, but downhills save a lot, which is why supercapacitor charging is used on downhills, while the battery is charged via the fuel cell only when the supercapacitor does the traction itself. Nevertheless, the simulation showed that both trains can overcome such a railway track and at the same time find the lowest energy consumption with different hybridization parameters.

The idle power of the fuel cell and the diesel engine has a big impact. The fuel cell at idle uses 6% of the nominal power, while the diesel engine uses as much as 20%, which greatly affects fuel consumption.

The lifetime of a railway vehicle depends on the installed equipment. Power sources and equipment are the same in HDEMU and HFCMU except for the main power source. The HDEMU is powered by a diesel engine, the HFCMU by fuel cells. The diesel engine requires more frequent overhaul intervals, which include oil, fluid and filter changes, and a major overhaul interval is 20 000 operating hours. The lifetime of the fuel cell is at least 10 000 operating hours, after which the fuel cell will be disassembled and the materials recycled. Other common power devices for HDEMU and HFCMU are shown in Tab. 3.

Table 4 Lifespan and overhaul interval of train power devices.

	Overhaul interval / hours	Lifespan
Diesel engine	20 000	-
Alternator	40 000	-
Inverter		20 years
Converter		20 years
Battery		12 years
Supercapacitor		1M cycles
Fuel cell		10 000 hours

HFCMU is more energy efficient than HDEMU and does not have harmful exhaust gas emissions. Hydrogen fuel cell technology provides a high-density source of energy with good energy efficiency. Hydrogen has the highest energy content of any common fuel by weight. Hydrogen is a perfectly clean fuel, because the only waste

produced by fuel cells is water vapor, while a diesel engine emits carbon dioxide and nitrogen oxides. HFCMU does not produce noise pollution like HDEMU.

Hydrogen does not exist on Earth, so it must be produced from other sources. The production requires a significant amount of energy, which is often obtained from fossil fuels, which undermines the environmental characteristics of hydrogen. But also, it is possible to produce hydrogen by solar power in PV cells. Fuel cells need significant investment to develop and are currently more expensive than a diesel engine. The storage and transport of hydrogen is more complex than that required for fossil fuels. It must not be forgotten that Hydrogen is highly flammable, which leads to understandable safety problems.

In future work, it is planned to add a photovoltaic cell as a power source in the energy distribution, and then the power sources can also be optimized.

15 REFERENCES

[1] IEA (2019). The Future of Rail: Opportunities for energy and the environment.

[2] Dimoula, V., Kehagia, F., & Tsakalidis, A. (2016). A Holistic Approach for Estimating Carbon Emissions of Road and Rail Transport Systems. *Aerosol and Air Quality Research*, *16*, 61-68. https://doi.org/10.4209/aaqr.2015.05.0313

[3] Mauch, A., Tophoven, J., Trzebiatowski T., &Raatz, T. (2011). Potentials and Limits of Downsizing a Diesel Engine. *MTZ Worldwide*, *72*(7-8), 4-9. https://doi.org/10.1365/s38313-011-0069-2

[4] Schimke, R. (2012). *Optimierung des Betriebsverhaltens und der Konfiguration von dieselelektrischen Lokomotiven*. Dissertation, Technische Universität Dresden.

[5] Andersen, C., Christensen M., & Korsgaard, A. (2002). *Design and Control of Fuel Cell System for Transport Application*. Project Group: EMSD 10 - 11A, Aalborg University.

[6] Guo, Y., Dai, X., Jermsittiparsert, K., & Razmjooy, N. (2020). An optimal configuration for a battery and PEM fuel cell-based hybrid energy system using developed Krill herd optimization algorithm for locomotive application. *Energy Reports*, *6*, 885-894. https://doi.org/10.1016/j.egyr.2020.04.012

[7] Shang, W., Yu, S., Zhang, G., Li Q., & Chen, W. (2017). Fuel cell hybrid locomotive system based on equivalent consumption minimization strategy. *Chinese Automation Congress (CAC)*, 2457-2461. https://doi.org/10.1109/CAC.2017.8243188

[8] Sarma, U. & Ganguly, S. (2018). Modelling and cost-benefit analysis of PEM fuel-cell-battery hybrid energy system for locomotive application. *Technologies for Smart-City Energy Security and Power (ICSESP)*, 1-5. https://doi.org/10.1109/icsesp.2018.8376691

[9] Khodaparastan, M. & Mohamed, A. (2017). Supercapacitors for electric rail transit systems. *IEEE 6th International Conference on Renewable Energy Research and Applications (ICRERA)*, 896-901. https://doi.org/10.1109/icrera.2017.8191189

[10] Lahyani, A., Venet, P., Guermazi A., & Troudi, A. (2013). Battery/Supercapacitors Combination in Uninterruptible Power Supply (UPS). *IEEE Transactions on Power Electronics*, *28*(4), 1509-1522. https://doi.org/10.1109/tpel.2012.2210736

[11] Furuta, R., Kawasaki J., & Kondo, K. (2010). Hybrid Traction Technologies with Energy Storage Devices for Nonelectrified Railway Lines. *IEEJ Transactions on Electrical and Electronic Engineering*, *5*(3), 291-297. https://doi.org/10.1002/tee.20532

[12] Serdar, J., (1977). *Lokomotive - opci dio*. Sveucilisna naklada Liber, Zagreb, Hrvatska.

[13] Arikan, Y., Şen T., & Çam, E. (2021). Energy Efficiency in Rail Systems with Coasting Control Method Using GA and ABC Optimizations. *Tehnički vjesnik*, *28*(4). https://doi.org/10.17559/TV-20200511115919

[14] Arajo, R. E. (2012). *Induction Motors - Modelling and Control*. Intech Open Limited, London, UK. https://doi.org/10.5772/2498

[15] Shi, W., Stapersma D., & Grimmelius, H. T. (2009). Analysis of energy conversion in ship propulsion system in off-design operation conditions. *Energy and Sustainability*, *1*, 461-472. https://doi.org/10.2495/ESU090411

[16] Kim, H.-S., Ryu, M.-H., Baek J., & Jung, J.-H. (2013).High-Efficiency Isolated Bidirectional AC-DC Converter for a DC Distribution System. *IEEE Transactions on Power Electronics*, *28*(4), 1642-1654. https://doi.org/10.1109/tpel.2012.2213347

[17] Sehrili, E. & Cetinceviz, Y. (2022). Comparasion of Average Curent Controlled PFC SEPIC and CUK Converter Feeding Current Controlled SRM. *Tehnički vjesnik*, *29*(6), 1789-1795. https://doi.org/10.17559/TV-20181108110207

[18] Lai, C.-M. (2016). Development of a Novel Bidirectional DC/DC Converter Topology with High Voltage Conversion Ratio for Electric Vehicles and DC-Microgrids. *Energies*, *9*(6), 410. https://doi.org/10.3390/en9060410

[19] MAN diesel engines for railvehicles (2008). MAN Nutzfahrzeuge AG, Nürnberg, Germany.

[20] Petrović, I., Hederić, Ž., Stojkov M., & Samardžić, I. (2021). Diesel Engine Selection on Locomotive Using AHP Methods. *Tehnicki vjesnik*, *28*(6), 2102-2108. https://doi.org/10.17559/tv-20210104211621

[21] Neudorfer, H., (2008). Entwicklung eines flüssigkeitsgekühlten Traktions-Synchrongenerators in Permanentmagnet-Technologie. *38. Tagung "Moderne Schienenfahrzeuge"*.

[22] Chen, W., Han, Y., Li, Q., Liu Z., & Peng, F. (2014). Design of proton exchange membrane fuel cell grid-connected system based on resonant current controller. *International Journal of Hydrogen Energy*, *39*(26), 14402-14410. https://doi.org/10.1016/j.ijhydene.2014.02.103

[23] Xiao Y. & Agbossou, K. (2009). Interface Design and Software Development for PEM Fuel Cell Modeling Based on Matlab/Simulink Environment. *WRI World Congress on Software Engineering*, 318-322. https://doi.org/10.1109/wcse.2009.344

[24] Meng, G., Wu, C., Zhang, B., Xue, F., & Lu, S. (2022). Net Hydrogen Consumption Minimization of Fuel Cell Hybrid Trains Using a Time-Based Co-Optimization Model. *Energies*, *15*(8), 2891. https://doi.org/10.3390/en15082891

[25] Saw, L., Somasundaram, K., Ye, Y., & Tay, A. (2014). Electro-thermal analysis of Lithium Iron Phosphate battery for electric vehicles. *Journal of Power Sources*, *249*, 231-238. https://doi.org/10.1016/j.jpowsour.2013.10.052

[26] Tremblay, O., Dessaint, L., & Dekkiche, A. (2007). A Generic Battery Model for the Dynamic Simulation of Hybrid Electric Vehicles. *IEEE Vehicle Power and Propulsion Conference*. https://doi.org/10.1109/vppc.2007.4544139

[27] Singha Roy, P. K., Karayaka, H., He, J., & Yu, Y. (2021). Economic Comparison between Battery and Supercapacitor for Hourly Dispatching Wave Energy Converter Power. *52nd North American Power Symposium*. https://doi.org/10.1109/NAPS50074.2021.9449677

Contact information:

Mario MIŠIĆ, PhD Student
(Corresponding author)
University of Slavonski Brod,
Mechanical Engineering Faculty in Slavonski Brod,
Trg Ivane Brlić Mažuranić 2, 35000 Slavonski Brod, Croatia
E-mail: mario.misic@yahoo.com

Marinko STOJKOV, PhD
University of Slavonski Brod,
Mechanical Engineering Faculty in Slavonski Brod,
Trg Ivane Brlić Mažuranić 2, 35000 Slavonski Brod, Croatia
E-mail: mstojkov@unisb.hr

Rudolf TOMIĆ, PhD
Faculty of Mechanical Engineering and Naval Architecture,
University of Zagreb,
Ivana Lucića 5, 10000 Zagreb, Croatia
E-mail: rudolf.tomic@fsb.hr

Mario LOVRIĆ, PhD Student
University of Slavonski Brod,
Mechanical Engineering Faculty in Slavonski Brod,
Trg Ivane Brlić Mažuranić 2, 35000 Slavonski Brod, Croatia
E-mail: mario.lovric2@gmail.com